Progress In Electromagnetics Research M, Vol. 114, 69–78, 2022

Design of an Ultra-Broadband Polarization Rotating Reflective Surface for the Reduction of Radar Cross Section

Xin Mu*, Miao Lv, and Tao Ni

Abstract—A novel ultra-broadband Polarization Rotation (PR) Reflective Surface (PRRS) is presented, which can reflect the linearly polarized incident wave in orthogonal polarization state. The proposed PRRS consists of a periodic array of double split ring patches printed on a substrate, which is backed by a metallic ground. A PRRS composed of circular split ring units can realize polarization rotation in two wide frequency bands. When two circular split rings with gradual radii are arranged concentrically, an ultra-broadband polarized rotation will be obtained. This paper explains the mechanism of polarization rotation and the mechanism of Radar Cross Section (RCS) reduction and studies the influence of structural parameters on the polarization rotation frequency band. Simulation results show that a 101.6% PR bandwidth is achieved. Meanwhile, by arranging the unit cells of the PRRS in four orthogonal directions, the monostatic RCS reduction band ranges from 8 GHz to 21.8 GHz (or 92.6%) for arbitrary polarization of the incident wave.

1. INTRODUCTION

Stealth is a military technology that improves its own survivability by changing the target feature information, reducing the interception probability of the enemy detection system, or shortening its discovery distance. At present, the stealth technology often mentioned by people generally refers to radar stealth technology. This technology mainly reduces Radar Cross Section (RCS) by the ingenious design of structure and shape or coating of absorbing materials.

In the last years, a number of new techniques for RCS reduction have been reported. The Electromagnetic Band Gap (EBG) structures and Artificial Magnetic Conductors (AMC) are the most commonly used for RCS reduction. Within the operation frequency band of an EBG or AMC, the reflections from the EBG or AMC and the Perfect Electric Conductor (PEC) or the antenna share the same magnitude but opposite phases. By combining the EBG or AMC and PEC in a chessboard-like configuration, these two reflections cancel each other under a normal incident plane wave, thus reducing the RCS in the normal direction is achieved [1–6]. In [1], a triangle type checker-board surface was reported to reduce the RCS of a planar surface. The RCS reduction bandwidth was from 59 GHz to 73 GHz (21.2%). A coding diffuse metasurface was proposed in [2] based on ergodic algorithm optimization. The metasurface provided the RCS reduction bandwidth from 5.4 GHz to 7.4 GHz (31.25%). Zhang et al. [3] developed an AMC based metasurface with the help of a circular ring structure with a parasitic cross within it. The dimensions of the unit cells were varied to obtain the required phase difference. The RCS reduction was observed from 8.2 to 10.25 GHz (22.22%) which exhibited narrowband performance. In [4], a structure consisted of a combination of a single band and dual band AMC unit cells with $180 \pm 37^\circ$ phase difference from 4.06 GHz to 11.2 GHz. RCS reduction compared to PEC surface was realized from 4.4 GHz to 11.68 GHz (91%).

Received 27 June 2022, Accepted 14 October 2022, Scheduled 26 October 2022
* Corresponding author: Xin Mu (jupitermx@126.com).
The authors are with the Xi'an Research Institute of Navigation Technology, Xi'an 710068, Shaanxi, P. R. China.

Phase Gradient Metasurface (PGM) used for wideband RCS reduction has also been researched in recent years. PGM can provide additional wave components along two in-plane directions simultaneously, leading to surface wave conversion, deflected reflection, or diffused reflection. There are several research studies on PGM for RCS reduction as well [5–7]. Li et al. [5] developed a two-dimensional phase gradient metasurface. The phase shifts in x and y directions were different, sub-unit cells with more variations were used, which can expand the bandwidth for RCS reduction from 7.5 GHz–12.2 GHz (47.7%).

Broadband Absorbing Materials (AMs) for RCS reduction have been proposed. AM is a practical approach utilized to decrease the RCS signature by means of converting the radio frequency energy into heat. Resistive and resistance-loaded absorbers can broaden the absorption band and enhance the absorptivity through multiple resonances [8]. Metamaterial structures presented in [8] obtained good absorbing performance in X-band using tailored unit cells in appropriate dimensions. The bandwidth of RCS reduction can reach 56.8%.

PRRS can reflect the linearly polarized incident wave with 90° polarization rotation. When the transmitter and receiver of the measurement system share the same polarized antenna, the monostatic RCS will be significantly reduced [9–17]. A two-grounded-via EBG structure and a quasi-L-shaped EBG structure were proposed in [9]. The PR bandwidths of the two structures reached 62% and 103.6%, and the RCS reduction bands were 5.5–8.25 GHz and 9.5 GHz–18.2 GHz. In a new approach, called Polarization Cancelation [10], the polarization of incident wave is rotated by several angles, so that the reflected wave becomes zero in direction of incidence. A 39% RCS reduction bandwidth was measured within the frequency band of 7.6 to 11.3 GHz.

Novel RCS reduction methods have been reported in the above literatures, but the bandwidth does not reach ultra-wideband. In this paper, a novel ultra-broadband PRRS for RCS reduction is presented. In [18], a transmission-type polarization converter with two separate operating frequency bands is obtained with a cut-wire sandwiched by two layers of a diagonal split-ring resonator (DSRR). After simulating the models mentioned in [18], it is found that when the electromagnetic wave irradiates the periodic structure composed of split rings, the polarization rotating will occur in both the transmitted wave and reflected wave. In this paper, a metal double circular split-rings patch structure is used to design the unit cell of the PRRS. The simulated and measured results show that the PR bandwidth of the proposed PRRS can reach 101.6%, and the monostatic RCS reduction band ranges from 8.2 GHz to 21.5 GHz (89.5%) for arbitrary polarization of the incident wave.

2. DESIGN OF THE CELL AND THE PRRS CONFIGURATION

A metal double circular split-rings patch structure is used to design the unit cell of the PRRS as shown in Fig. 1. The circular split ring metal patch consists of two annular metal patches with gradual radii. The small circular split ring is concentrically nested within the large split ring, and the split size and direction of each split ring are the same. A Rogers RT/duroid 5880 substrate with the dielectric constant $\varepsilon r = 2.2$ is chosen to design the PRRS unit cell. The height of the substrate is $h = 2$ mm. The substrate is backed by a metallic ground of copper. The unit cell has advantages in terms of its geometry, resonant frequency control, and polarization conversion characteristics. The parametric analysis is done in HFSS V15.0 software to arrive at the optimum dimensions of the unit cell. The geometry of the proposed PRRS is shown in Fig. 5.

The mechanism of the polarization rotation can be explained with the help of S-parameters theory. Ei is the incident electric field, and Er is the reflected electric field. Fig. 2 shows that Ei is decomposed into two orthogonal components. Eiu is a u-polarized incident electric field, and Eiv is a v-polarized incident electric field. Meanwhile, Eru is a u-polarized reflected electric field, and Erv is a v-polarized reflected electric field. Since PRRS is a lossless material, the incident wave has the same amplitude as the reflected wave. However, Erv and Eiv are opposite in phase. After the addition of Erv and Eru, the phase difference between Ei and Er is 90 degrees, and the amplitudes are the same. Therefore, the electromagnetic wave realizes polarization rotation after being reflected by PRRS.

We define S_{YY} to represent the amplitude of the reflection coefficient of the incident wave and the reflected wave polarized in the Y-direction, and S_{YX} to represent the amplitude of the reflection coefficient of the incident wave polarized in the Y-direction and the reflected wave in the X-direction.

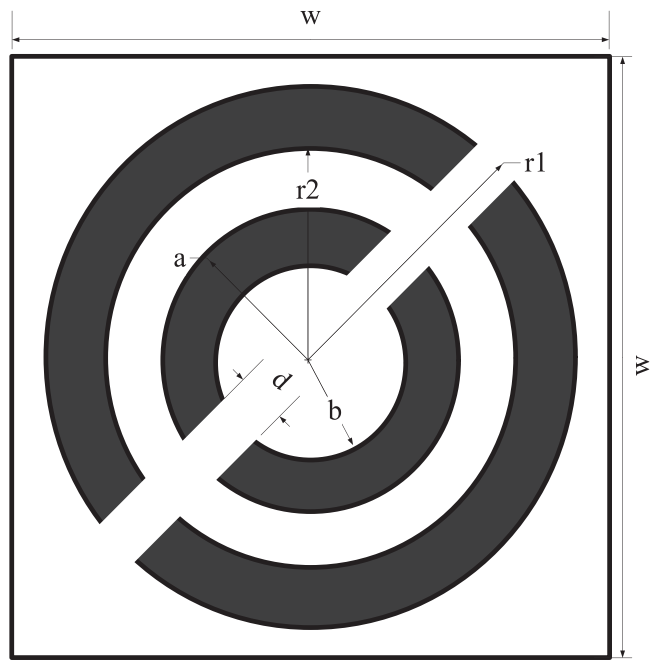

Figure 1. Front view of the PRRS unit cell.

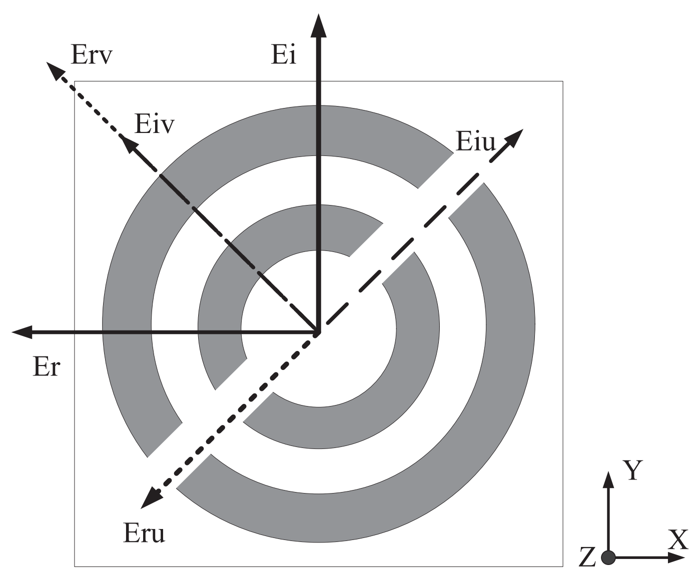

Figure 2. Mechanism of polarization rotation.

When the incident electromagnetic wave polarized in the Y-direction vertically irradiates the PRRS, S_{YY} and S_{YX} vary with frequency as shown in Fig. 3. It can be seen that the incident wave polarized in the Y direction becomes the reflected wave polarized in the X direction after being reflected by the PRRS.

Figure 4 explains the general mechanism of RCS reduction. The cells of PRRS with different orientations are divided into four parts. If the incident electric field Ei illuminates the PRRS, then the reflected electric fields generated by part 1 and part 2 are $Er1$ and $Er2$, respectively. $Er1$ and $Er2$ have the same amplitude but opposite phases, and they cancel each other out. So, whenever a wave is incident on the PRRS, the reflected fields from adjacent regions are cancelled, and the echo

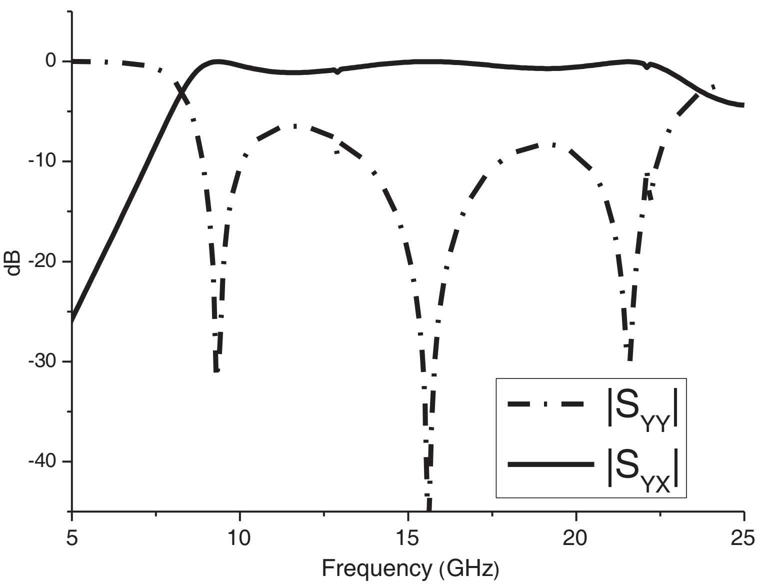

Figure 3. S_{YY} and S_{YX} varies with frequency.

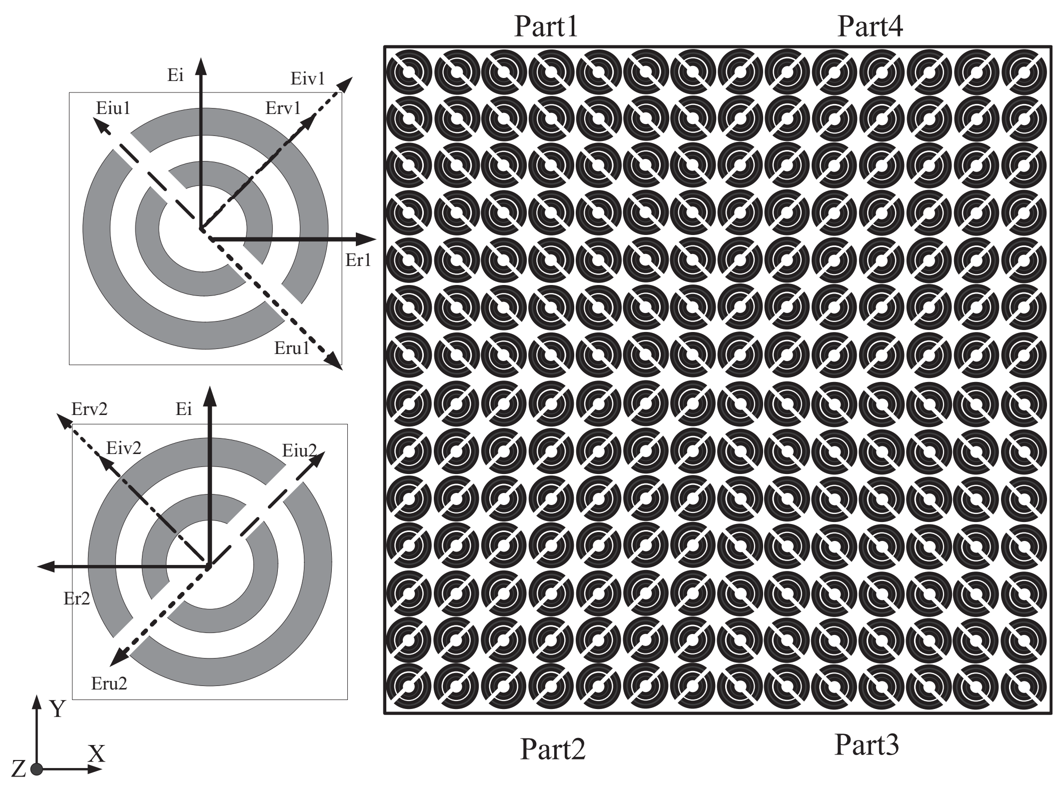

Figure 4. Mechanism of RCS reduction.

signal cannot reach the radar receiver resulting in excellent RCS reduction. The designed PRRS is a centro-symmetric structure, which has no relationship with the polarization direction of the incident wave. Therefore, the PRRS has the RCS reduction effect on electromagnetic waves polarized in any direction.

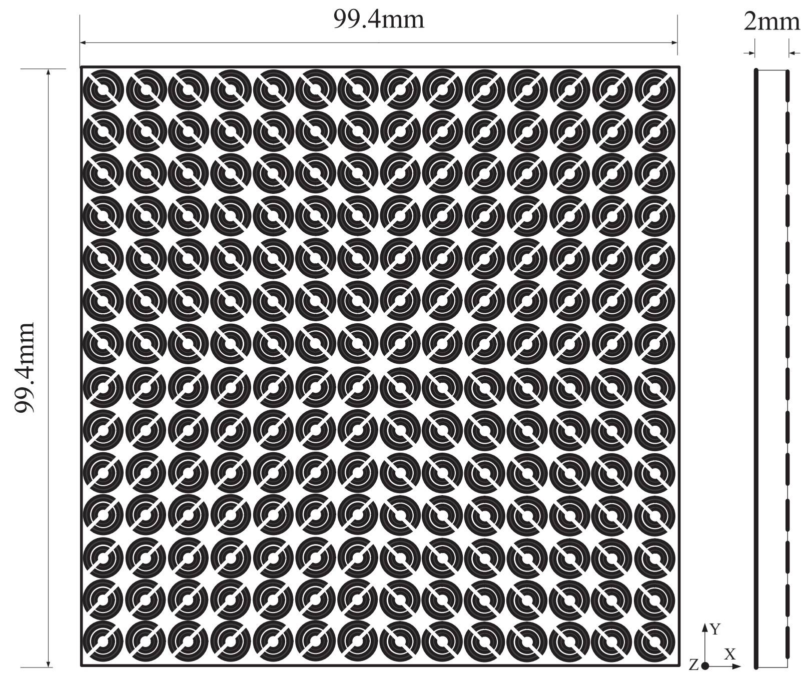

Figure 5. Geometry of the proposed PRRS.

3. RESULTS AND ANALYSIS

In the following, we define $r_{TE/TM} = E_{TM}^{Ref}/E_{TE}^{Ref}$ and $r_{TE/TE} = E_{TE}^{Ref}/E_{TE}^{Ref}$ to represent the reflection ratio of TE to TM, and TE to TE. So the Polarization Rotation Ratio (PRR) is defined as $PCR = |r_{TE/TM}|^2/(|r_{TE/TM}|^2 + |r_{TE/TE}|^2)$. E_{TE}^{Ref} represents the reflected electric field with the

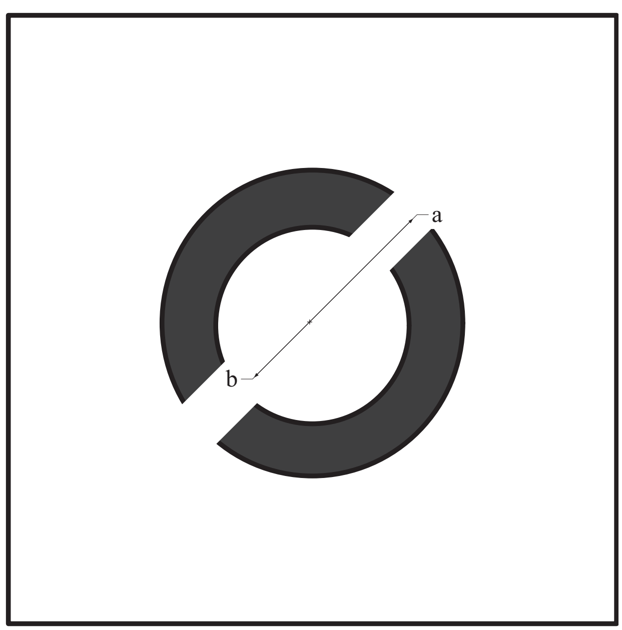

Figure 6. Front view of one split ring unit cell.

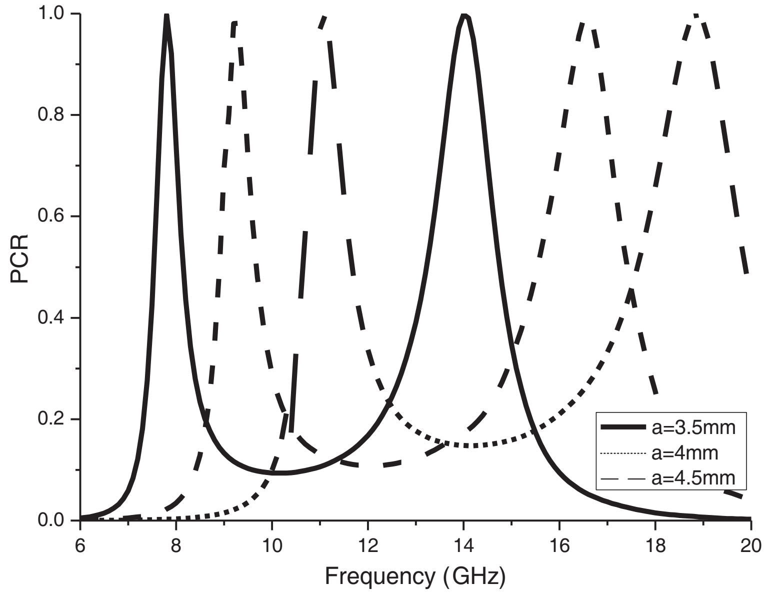

Figure 7. Simulated PRR with different a.

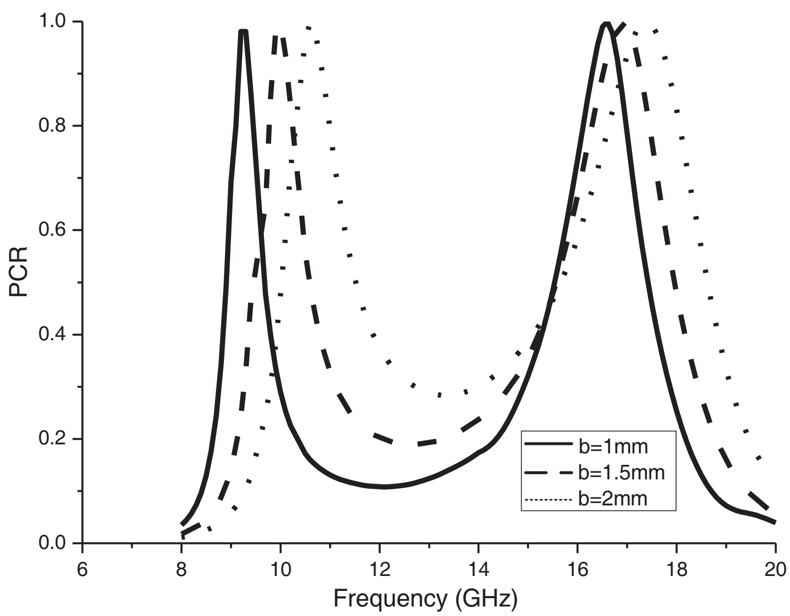

Figure 8. Simulated PRR with different b.

polarization direction in the X direction, and E_{TM}^{Ref} represents the reflected electric field with the polarization direction in the Y direction. The conclusion drawn from [8] is that the monostatic RCS in the normal direction is reduced by the PRR rather than other variables. In order to produce a wider PR band with high PRR, the parameters of the cells are optimized.

Firstly, the cell with only one circular split ring is simulated in Fig. 6. The inner radius and outer radius of the circular split ring are b and a. The simulation results are show in Fig. 7 and Fig. 8, and we can see that the PRR curves change intensely with a, while the PR frequency bandwidth is not changed. Moreover, it can be seen that the larger the b is, the wider the PCR bandwidth is in Fig. 8.

Secondly, based on the analysis above, a bigger circular split ring with inner radius $r2$ and outer radius $r1$ has been added in a smaller one to form double circular split rings. The bigger one will

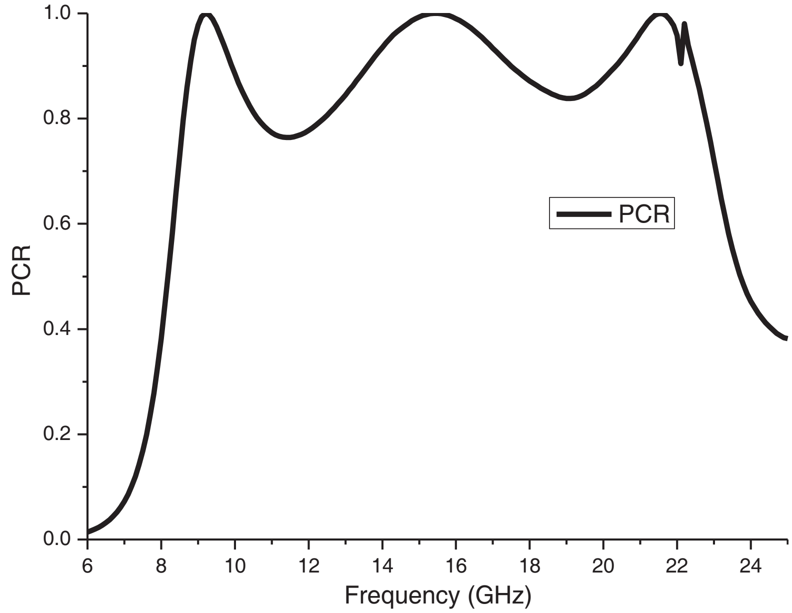

Figure 9. Simulated PRR of the PRRS with double split rings.

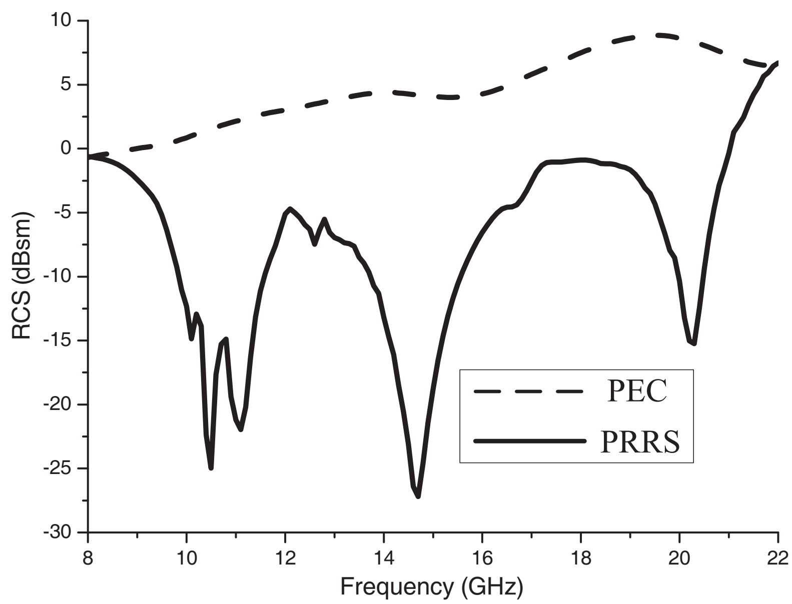

Figure 10. Simulated RCS of the proposed PRRS and metal plane.

enhance the PR bandwidth. The period of the unit cell w was set as 7.1 mm, and the gap of the split ring d was set as 1 mm. By optimizing the radius of the rings reasonably, an ultra-broadband PRRS will be obtained. Fig. 1 shows the structure of the cell, and Fig. 9 shows the simulated PRR of the proposed PRRS. The parameters of the PRRS are $w = 7.1$ mm, $r1 = 6.8$ mm, $r2 = 5$ mm, $a = 3.6$ mm, $b = 1.8$ mm, and $d = 1$ mm.

Lastly, the proposed PRRS was fabricated as shown in Fig. 11. The simulated and measured RCSs with different polarization directions of the PRRS compared with that of the PEC plane are given in Fig. 10 and Fig. 12. Experimental measurements of RCS were carried out in an anechoic chamber. Because of the limitations of the experimental measurement setup, the RCS measurements were carried out from 8–18 GHz. It can be seen that the RCS reduction bandwidth ranges from 8 GHz to 21.8 GHz.

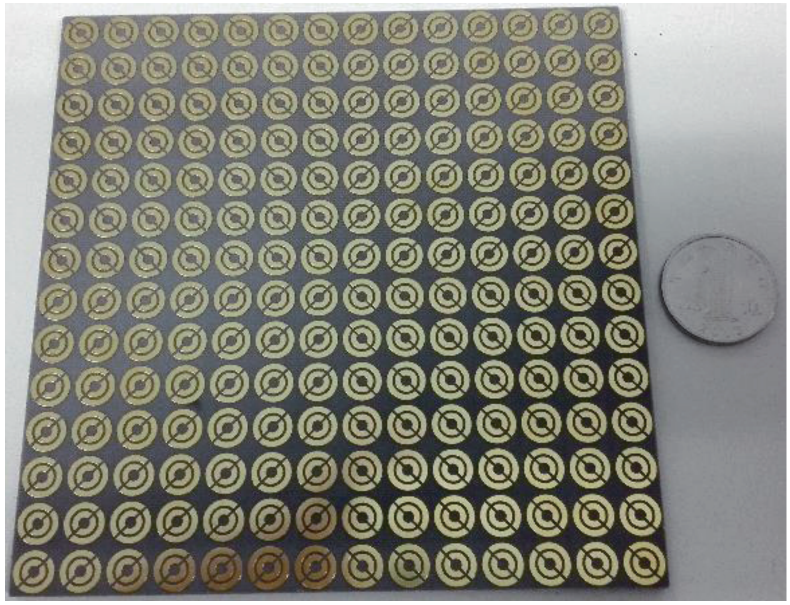

Figure 11. Photograph of proposed PRRS.

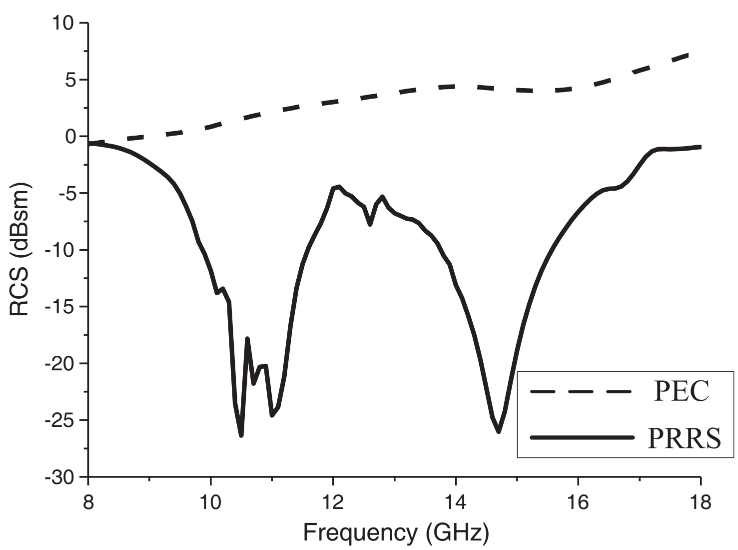

Figure 12. Measured RCS of the proposed PRRS and metal plane.

The simulated and experimentally measured results are in good agreement. Slight variations may be observed due to fabrication tolerances and limitations in the experimental measurement setup.

4. COMPARISON WITH PUBLISHED LITERATURE

Table 1 shows the advantages of the proposed design over the present state-of-the-art. The comparison is done in terms of features, methodology used, and percentage bandwidth of RCS reduction. It is observed from the comparison that most of the designs suffered from narrow bandwidth. The proposed design offers a wide RCS reduction bandwidth as compared with the other designs.

Table 1. Comparison of the proposed design with similar work.

Ref., Year of Publication	Methodology Used	Features	RCS reduction Bandwidth
Ref. [1] 2020	AMC	mmWave frequencies	59–73 GHz (21.2%)
Ref. [2] 2017	EBG or AMC	Coding diffuse metasurface	5.4–7.4 GHz (31.25%)
Ref. [3] 2018	AMC	Circular Ring with Parasitic Cross-AMC	8.2–10.25 GHz (22.22%)
Ref. [4] 2018	AMC	A combination of a single band and dual band AMC	4.4–11.68 GHz (91%)
Ref. [5] 2014	PGM	Two-dimensional phase gradient metasurface	7.5–12.2 GHz (47.7%)
Ref. [8] 2013	AM	Resistive and resistance-loaded absorbers	56.8%
Ref. [9] 2016	PRRS	Asymmetric EBG structure	5.5–8.25 GHz and 9.5–18.2 GHz
Ref. [10] 2018	PRRS	Polarization Cancelation	7.6–11.3 GHz (39%)
Proposed Design	PRRS	Bouble circular split-rings patch structure	8.2–21.5 GHz (92.6%)

5. CONCLUSION

A novel ultra-wideband PRRS for the reduction of RCS is presented and measured. A metal double circular split-rings patch structure is used to design the unit cell of the PRRS. A PRRS composed of circular split ring units can realize polarization rotation in two wide frequency bands. When two circular split rings with gradual radii are arranged concentrically, an ultra-broadband polarized rotation will be obtained. Simulation results show that a 101.6% PR bandwidth is achieved. We arrange the unit cells of the PRRS in four orthogonal directions and fabricate it. Ultra-broadband RCS reduction is achieved by the mutual cancellation of reflected waves generated by the four parts. The simulated and measured result show that the RCS reduction bandwidth ranges from 8 GHz to 21.8 GHz (or 92.6%). The proposed PRRS offers a wide RCS reduction bandwidth compared with the other designs.

The PRRS proposed in this paper can be applied in many fields such as antenna RCS reduction, improvement of aircraft stealth level, and improvement of electromagnetic compatibility. Future research includes changing the shape of the split rings to further increase the RCS reduction bandwidth.

REFERENCES

1. Samadi, F. and A. Sebak, "Dielectric based triangle-type AMC structure for RCS reduction at mmWave frequencies," *IEEE International Symposium on Antennas and Propagation and North American Radio Science Meeting*, 1193–1194, 2020.
2. Liu, X., J. Gao, L. Xu, X. Cao, Y. Zhao, and S. Li, "A coding diffuse metasurface for RCS reduction," *IEEE Antennas and Wireless Propagation Letters*, Vol. 16, 724–727, 2017.
3. Zhang, X. L., M. Niu, L. H. Su, and K. P. Song, "Radar cross section reduction based on metasurface," *ChinaCom 2017: Communications and Networking, Lecture Notes of the Institute for Computer Sciences, Social Informatics and Telecommunications Engineering*, B. Li, L. Shu, D. Zeng (eds.), 236, Springer, Cham, 2018.

4. LibiMol, V. A. and C. K. Aanandan, "Wideband radar cross section reduction using artificial magnetic conductor checkerboard surface," *Progress In Electromagnetics Research M*, Vol. 69, 171–183, 2018.
5. Li, Y. F., J. Q. Zhang, S. B. Qu, J. F. Wang, H. Y. Chen, Z. Xu, and A. X. Zhang, "Wideband radar cross section reduction using two-dimensional phase gradient metasurface," *Appl. Phys. Lett.*, Vol. 104, 221110, 2014.
6. Kumar, P. V. and B. Ghosh, "Polarization sensitive dual-band metasurface lens for X-band applications," *Progress In Electromagnetics Research M*, Vol. 103, 141–149, 2021.
7. Joy, V., A. Dileep, P. Abhilash, R. U. Nair, and H. Singh, "Metasurfaces for stealth applications: A comprehensive review," *Journal of Electronic Materials*, 1–20, 2021.
8. Turpin, J. P., P. E. Sieber, and D. H. Werner, "Absorbing ground planes for reducing planar antenna radar cross-section based on frequency selective surfaces," *IEEE Antennas Wireless Propag. Lett.*, Vol. 12, 1456–1459, 2013.
9. Jia, Y., Y. Liu, Y. J. Guo, K. Li, and S.-X. Gong, "Broadband polarization rotation reflective surfaces and their applications to RCS reduction," *IEEE Transactions on Antennas and Propagation*, Vol. 64, No. 1, Jan. 2016.
10. Khalaj-Amirhosseini, M. and M. Khanjarian, "Radar cross section reduction using polarization cancellation approach," *Progress In Electromagnetics Research Letters*, Vol. 74, 107–110, 2018.
11. Yang, W., K.-W. Tam, W.-W. Choi, W. Che, and H. Hui, "Polarization rotation reflective surface based on artificial magnetic conductor and its application," *Electronics Letters*, Vol. 50, No. 21, 2015.
12. Ghosh, S., S. Bhattacharyya, D. Chaurasiya, and K. V. Srivastava, "An ultrawideband ultrathin metameterial absorber based on circular split rings," *IEEE Antenna and Wireless Propagation Letters*, Vol. 14, 2015.
13. Patel, K. and M. Joshi, "Broadband radar cross section reduction of microstrip antenna using polarization conversion metasurface," *Progress In Electromagnetics Research B*, Vol. 96, 67–86, 2022.
14. Qi, Y., B. Zhang, C. Liu, and X. Deng, "Ultra-broadband polarization conversion meta-surface and its application in polarization converter and RCS reduction," *IEEE Access*, Vol. 8, 116675–116684, 2020.
15. Murugesan, A., K. T. Selvan, A. K. Iyer, K. V. Srivatsav, and A. Alphones, "A review of metasurface-assisted RCS reduction techniques," *Progress In Electromagnetics Research B*, Vol. 94, 75–103, 2021.
16. Yin, J. Y., H. J. Sun, and L. Zhang, "An ultra-wideband polarization conversion meta-surface and its application in RCS reduction," *Progress In Electromagnetics Research Letters*, Vol. 89, 29–36, 2020.
17. Khalaj-Amirhosseini, M. and M. Khanjarian, "Radar cross section reduction using polarization cancellation approach," *Progress In Electromagnetics Research Letters*, Vol. 74, 107–110, 2018.
18. Zhao, R., H. Chen, L. Zhang, F. Li, P. Zhou, J. Xie, and L. Deng, "Design and implementation of high efficiency and broadband transmission-type polarization converter based on diagonal split-ring resonator," *Progress In Electromagnetics Research*, Vol. 161, 1–10, 2018.